DR AAMER SAEED (Orcid ID : 0000-0002-7112-9296)

MR. FAYAZ ALI LARIK (Orcid ID : 0000-0002-8491-5229)

Article type : Research Article

Extending the scope of amantadine drug by incorporation of phenolic azo Schiff bases as potent selective inhibitors of carbonic anhydrase II, drug likeness and binding analysis

Pervaiz Ali Channar[a] Aamer Saeed*[a], Danish Shahzad[a], Fayaz Ali Larik*[a], Mubashir Hassan[b], Hussain Raza[b], Qamar Abbas[c], Sung-Yum Seo[b]

[a] *Department of Chemistry, Quaid-I-Azam University, Islamabad 45320, Pakistan*

[b]*Department of Biological Sciences, College of Natural Sciences, Kongju National University, 56 Gongjudehak-Ro, Gongju, Chungnam 32588, Republic of Korea*

[c]*Department of Physiology, University of Sindh, Jamshoro-76080, Pakistan*

* Email: aamersaeed@yahoo.com, fayazali@chem.qau.edu.pk (F.A.L) Tel +92-51-9064-2128; Fax: +92-51-9064-2241

This article has been accepted for publication and undergone full peer review but has not been through the copyediting, typesetting, pagination and proofreading process, which may lead to differences between this version and the Version of Record. Please cite this article as doi: 10.1111/cbdd.13335

Abstract

A series of Amantadine based azo Schiff base dyes **6a-6e** have been synthesized and characterized by ^{1}H NMR and ^{13}C NMR and evaluated for their *in vitro* carbonic anhydrase II inhibition activity and antioxidant activity. All of the synthesized showed excellent carbonic inhibition. Compound **6b** was found to be the most potent derivative in the series, the IC_{50} of **6b** was found to be 0.0849 ± 0.00245µM (standard Acetazolamide IC_{50}=0.9975±0.049µM). The binding interactions of the most active analogs were confirmed through molecular docking studies. Docking studies showed **6b** is interacting by making two hydrogen bonds w at His93 and Ser1 residues respectively. All compounds showed a good drug score and followed Lipinski's rule. In summary, our studies have shown that these amantadine derived phenolic azo Schiff base derivatives are a new class of carbonic anhydrase II inhibitors.

Keywords: Amantadine Drug derivatives; phenolic azo Schiff bases; Carbonic anhydrase II inhibition; antioxidant; Drug Score; Drug likeness; Binding analysis

1. Introduction

1-Adamantylamine is commercially known as amantadine and it contains adamantine as a backbone and has one amine group along with four methylene groups [1]. Amantadine is an antiviral and antiparkinsonian drug and particularly inhibits influenza A virus [2]. Moreover, Amantadine also blocks calcium channel protein Kcv and also it assists in releasing of dopamine [3, 4]. Apart from being the medicinally significant drug, amantadine serves as the key precursor for incorporation of the adamantine skeleton inorganic compounds [5].

The carbonic anhydrase enzyme represents a broad class of metallo-enzymes and widely distributed among mammals [6]. There are 15 isoforms of carbonic anhydrase are known and this

enzyme catalyzes the cleavage of carbon dioxide [7]. The isoforms of carbonic anhydrase are categorized into two categories i) systolic (CA I, CA II, CA III, CA VII and CA XIII) ii) Membrane-bound (CA IV, CA IX, CA XII, and CA XIV). Carbonic anhydrase (CA, EC 4.2.1.1) inhibitors (CAIs) for isoforms I-II (glaucoma associated) and IX-XII (cancer-associated) [8]. Carbonic anhydrase (CA) plays an important role in the regulation of respiration, bone resorption, pH regulation and CO2 homeostasis, tumorigenicity and these features ignite medicinal chemists to search efficient and safe carbonic anhydrase inhibitors (CAI) since the 1950's[9, 10]. Carbonic anhydrase contains Zn^{+2} ion as Lewis acid which assists in binding of the active substrate with the water molecule. Zn^{+2} is tightly bound with three histidine units [11]. The nucleophilic oxygen of water molecule attacks the electrophilic carbon of carbon dioxide to form the complex with zinc ions which then collapse to release bicarbonate ions (Figure 1).

<<Insert Figure 1>>

A large number of sulfonamide based carbonic anhydrase inhibitor (CAI) drugs like are in clinical use for more than 70 years as diuretics, antiglaucoma, anticonvulsant or anti-infective drugs examples of clinically used CAIs: acetazolamide AZM, methazolamide MZA, ethoxzolamide EZA, dorzolamide DZA, brinzolamide BRZ, zonisamide ZNS, sulpiride SLP, indisulam IND, celecoxib CLX (Figure 2)[12-14].

<<Insert Figure2>>

However, due to numerous isoform of carbonic anhydrase enzyme, the search to obtain effective safe drug candidates is still work in progress.

Schiff bases possess the broad spectrum of biological activities antibacterial, antifungal, anti-mouse hepatitis virus (MHV), inhibition of herpes simplex virus type 1 (HSV-1) and adenovirus type 5 (Ad 5), anticancer, anti-mosquito larvae and herbicidal activities [15-17]. Moreover Schiff base is important precursors in the synthesis of β-lactams and metal complexes [18]. It is assumed that the azomethine moiety in Schiff bases is responsible for biochemical interactions. Azo compounds possess academic and industrial important and are considered as building blocks in the synthesis of metal complexes and polymers [19, 20]. Moreover, azo compounds possess biological importance such as inhibition of DNA, RNA, and protein synthesis, nitrogen fixation, and carcinogenesis [21].

Hybrid pharmacophore approach has been considered as the hallmark in seeking potent derivatives in chemical bio drug designing. In this account, we have a hybrid pharmacophore based strategy to design potent carbonic anhydrase (CA II) inhibitors). Amantadine drug was chosen as core skeleton and it was linked with azo and Schiff base moieties to incorporate intriguing structural features. Schiff bases contain imine moiety and are known as masked carbonyl analogue of either aldehyde or ketone. The azo group exhibits diverse applications in material chemistry has been induced as linked with amantadine drug. The hydroxyphenyl ring was suitably substituted with various electronic perturbing groups in order to investigate the role of substituents attached to the aryl ring. Herein, we have chosen free amino-containing amantadine drug to extend it's by incorporating phenolic azo Schiff bases and the synthesized derivatives were screened against carbonic anhydrase II enzyme inhibition and using molecular simulation drug score, drug-likeness and binding analysis were explored.

2. Experimental

2.1 Methods and Materials

The R_f values were determined using aluminum precoated silica gel plates Kiesel 60 F254 from Merck (Germany). Melting points of the compounds were measured in open capillaries using Stuart melting point apparatus (SMP3) and are uncorrected. ^{1}H-NMR spectra were determined as DMSO, $CDCl_3$ solutions at 300 MHz using a Bruker AM-300 spectrophotometer, and the ^{13}C-NMR spectra were determined at 75 MHz using a Bruker 75 MHz NMR in DMSO-d6, and $CDCl_3$ solutions. The elemental analysis was performed on Leco CHNS-932 Elemental Analyzer (Leco Corporation, USA). For the synthesis of compounds, all chemicals were commercially obtained and used without additional purification.

2.2 General procedure for synthesis of phenolic azo dyes (4a-3e) and their condensation with Amantadine hydrochloride (5)

Suitably substituted anilines **(1a-1e)** (0.01mol) were dissolved in 20ml water and 3.5ml concentrated HCl, with stirring maintaining the temperature at 0-5^{o}C. A solution of $NaNO_3$ (0.01ml) in 10ml water was added promptly to the solution of aniline with continuous and vigorous stirring. Stirring was further continued for 1h maintaining the temperature in the same range. After 1h the reaction mixture was checked for the completeness of reaction on a paper chromatogram using water as mobile phase. The dried chromatogram was sprayed with the solution of *p-N, N*-dimethyl amino benzaldehyde in ethanol as spraying agent. On completion of the reaction, the diazonium salts **(2a-2e)** were kept in the freezer.

Salicylaldehyde (0.01ml) was dissolved in water (15ml) and K_2CO_3 (1.5g), kept in an ice bath at temperature 0-5^{o}C with stirring. The diazo solution was added dropwise to the stirred solution of salicylaldehyde during 45 minutes, maintaining the pH above 8. The progress of the reaction was

monitored by paper chromatography using H-acid solution in alkaline media. On completion, the solids were filtered, dried in the oven at 70^{o}C, for 3hs to afford the 4-(Benzeneazo) salicylaldehyde derivatives **(4a-4e)** in 85-92% yields. In the case where regioisomeric products were obtained; column chromatography was used for separation. Then 0.01mol (0.5g) amantadine hydrochloride **5** was slowly added to a solution of 0.01 mol of 4-(Benzeneazo) salicylaldehyde derivatives 0.002mol **(4a-4e)**. After refluxing the reaction mixture for 3h, the precipitate was cooled and collected by filtration. The precipitate was washed several times using ethanol, followed by crystallization in ethanol and drying at 50 ^{o}C overnight. Yields > 70%.

2-((*E*)-((3s,5s,7s)-Adamantan-1-ylimino)methyl)-4-((*E*)-(4-chlorophenyl)diazenyl)phenol (6a)

Dark yellow solid, M.P=240^{o}C, Yield 88%, $R_{f=}$ 0.50 (Chloroform: Ethanol 9:1), ^{1}H NMR ($CDCl_3$, 300 MHZ); δ (ppm) 11.29 (s, 1H, Ar-OH), 9.61 (s, 1H, =N-CH), 8.14 (d,1H, Ar-H, *J*= 2.4Hz), 8.15 (d, 1H, Ar-H, *J*= 1.97Hz), 8.08 (dd, 1H, Ar-H, *J*=8.4, *J*=2.3Hz), 7.89-7.51 (m, 4H, Ar-H), 7.17 (d, 1H, Ar-H, *J*=7.4Hz), 2.06 (m, 3H), 1.71 (m, 6H), 1.60 (m, 6H), ^{13}C NMR (75 MHz $CDCl_3$) δ (ppm), ^{13}C NMR (75 MHz DMSO-d6) δ (ppm), 188.05 (OH-C), 163.74, 151.88, 150.46, 145.15, 130.21, 127.14, 124.33, 123.09, 122.39, 118.89, 65.5, 51.47, 35.48, 28.75; found: C, 70.11; H, 6.09; N, 10.6.

4-((*E*)-(3-((*E*)-((3s,5s,7s)-Adamantan-1-ylimino)methyl) 4-hydroxyphenyl)diazenyl)benzenesulfonamide (6b)

Dark orange crystalline solid, M.P=240^{o}C, Yield 88%, $R_{f=}$ 0.70 (Chloroform: Ethanol 9:1),^{1}H NMR (DMSO-d_6, 300 MHZ); δ (ppm) 11.52 (s, 1H, Ar-OH), 10.35 (s, 1H, =N-CH), 8.18 (d,1H, Ar-H, *J*= 2.5Hz), 8.11 (dd, 1H, Ar-H, *J*=8.7, *J*=2.4Hz), 7.80 (m, 4H, Ar-H), 7.53 (s, 4H), 7.20 (d,

1H, Ar-H, *J*=7.5Hz), 2.07 (m, 3H), 1.74 (m, 6H), 1.59 (m, 6H)**,** ^{13}C NMR (75 MHz DMSO-d6) δ (ppm), ^{13}C NMR (75 MHz DMSO-d6) δ (ppm), 190.05 (OH-C), 162.84, 151.91, 150.94, 145.21, 130.23, 127.16, 124.31, 123.09, 122.39, 118.89, 65.52, 51.47, 35.48, 28.75, Anal.Calcd. for $C_{23}H_{26}N_4O_3S$: C, 62.99; H, 5.98; N, 12.78; S, 7.31; found: C, 62.99; H, 5.98; N, 12.78; S, 7.31

Sodium-4-((*E*)-(3-((*E*)-((3s,5s,7s)-adamantan-1-ylimino)methyl)-4 hydroxyphenyl)diazenyl)benzenesulfonate (6c)

Dark yellow crystalline solid, M.P=240^{o}C, Yield 88%, $R_{f=}$ 0.60 (Chloroform: Ethanol 9:1), ^{1}H NMR (DMSO-d_6, 300 MHZ); δ (ppm) 11.54 (s, 1H, Ar-OH), 10.37 (s, 1H, =N-CH), 8.19 (d,1H, Ar-H, *J*= 2.5Hz), 8.11 (dd, 1H, Ar-H, *J*=8.7, *J*=2.4Hz), 7.80 (m, 4H, Ar-H), 7.21 (d, 1H, Ar-H, *J*=7.5Hz), 2.08 (m, 3H), 1.74 (m, 6H), 1.59 (m, 6H), ^{13}C NMR (75 MHz DMSO-d6) δ (ppm), 191.05 (OH-C), 163.84, 151.99, 150.94, 145.29, 130.26, 127.16, 124.33, 123.09, 122.39, 118.89, 65.53, 51.47, 35.48, 28.75, Anal.Calcd. for $C_{23}H_{24}N_3NaO_4S$: C, 59.86; H, 5.24; N, 9.10; S, 6.95 found: C, 59.81; H, 5.19; N, 9.02; S, 6.89.

2-((*E*)-((3s,5s,7s)-Adamantan-1-ylimino)methyl)-4-((*E*)-p-tolyldiazenyl)phenol (6d)

Light yellow solid, M.P=240^{o}C, Yield 88%, $R_{f=}$ 0.70 (n-Hexane: Ethyl acetate 6:4), ^{1}H NMR ($CDCl_3$, 300 MHZ); δ (ppm) 11.21 (s, 1H, Ar-OH), 9.49 (s, 1H, =N-CH), 8.14 (d,1H, Ar-H, *J*= 2.4Hz), 8.12 (d, 1H, Ar-H, *J*= 1.97Hz), 8.05 (dd, 1H, Ar-H, *J*=8.4, *J*=2.3Hz), 7.93, (dd, 4H, Ar-H, *J*=8.8Hz), 7.14 (d, 1H, Ar-H, *J*=7.4Hz), 2.34(s, 3H), 2.06 (m, 3H), 1.71 (m, 6H), 1.60 (m, 6H), ^{13}C NMR (75 MHz $CDCl_3$) δ (ppm), 186.05 (OH-C), 159.84, 151.99, 150.94, 145.22, 130.26, 127.16, 124.23, 123.03, 122.31, 118.89, 65.43, 51.44, 35.48, 28.75, 21.86, Anal.Calcd. for $C_{24}H_{27}N_3O$: C, 77.18; H, 7.29; N, 11.25: found: C, 77.12; H, 7.26; N, 11.21.

2-((*E*)-((3s,5s,7s)-Adamantan-1-ylimino)methyl)-4-((*E*)-((3-chlorophenyl)imino)methyl)phenol (6e)

Dark yellow solid, M.P=240^{o}C, Yield 88%, $R_{f=}$ 0.50 (n-Hexane: Ethyl acetate 6:4), ^{1}H NMR ($CDCl_3$, 300 MHZ); δ (ppm) 11.30 (s, 1H, Ar-OH), 9.63 (s, 1H, =N-CH), 8.14 (d,1H, Ar-H, *J*= 2.4Hz), 8.16 (d, 1H, Ar-H, *J*= 1.97Hz), 8.08 (dd, 1H, Ar-H, *J*=8.4, *J*=2.3Hz), 8.14-7.52 (m, 4H, Ar-H), 7.19 (d, 1H, Ar-H, *J*=7.4Hz), 2.07 (m, 3H), 1.73 (m, 6H), 1.60 (m, 6H), ^{13}C NMR (75 MHz $CDCl_3$) δ (ppm), 187.01 (OH-C), 163.68, 151.77, 150.34, 145.07, 130.22, 128.08, 129.06, 127.10, 124.33, 123.09, 122.39, 118.89, 65.5, 51.47, 35.48, 28.7 Anal.Calcd. for $C_{24}H_{25}ClN_2O$: C, 73.36; H, 6.41; N, 7.13; found: C, 73.30; H, 6.36; N, 7.09.

2.3 Carbonic anhydrase assay

Carbonic anhydrase inhibition was measured as described previously with some modifications [28]. The method is based on the principle that *p*-nitrophenyl acetate is hydrolyzed by Carbonic anhydrase to form yellow colored *p*-nitrophenol which was measured spectrophotometrically. Briefly, the Reaction mixture contained 120 µL of 50 mM Tris-sulfate buffer (pH 7.6 containing 0.1 mM $ZnCl_2$), 20 µL of inhibitor and 20 µL (50 U) bovine enzyme per well. Contents were well mixed and pre-incubated at 25 °C for 10 min. substrate *p*-nitrophenyl acetate was prepared (6 mM stock using <5% acetonitrile in the buffer and used fresh every time) and 40 µL was added per well to achieve 0.6 mM concentration per well. The total reaction volume was made to 200 µL. After 30 min incubation at 25 °C contents was mixed and absorbance was measured at 348 nm using a microplate reader. Acetazolamide was used as a reference inhibitor and Tris-sulfate buffer was used as negative control. Each concentration was analyzed in three

independent experiments. IC_{50} values were calculated by nonlinear regression using GraphPad Prism 5.0.

$$\text{Inhibition (\%)} = [(B - S)/B] \times 100$$

Here, the B and S are the absorbances for the blank and samples.

2.4 Repossession of Carbonic anhydrase II from PDB

The three dimensional (3D) crystal structure of carbonic anhydrase II was retrieved from the Protein Data Bank (PDB) having PDBID 1V9E (www.rcsb.org). Energy minimization of target structure was carried out by using conjugate gradient algorithm and Amber force field in UCSF Chimera 1.10.1[30]. The stereo-chemical properties, Ramachandran graph, and values of Carbonic anhydrase II structure were assessed by Molprobity server, while the hydrophobicity graph was generated by Discovery Studio 4.1 Client [31-33]. The protein architecture and statistical percentage values of helices, beta-sheets, coils, and turns were accessed by using online tool VADAR 1.8[34].

2.5 In-silico designing of synthesized compounds

The synthesized ligand molecules (6a-e) were sketched in drawing ACD/ChemSketch tool and further minimized by visualizing software UCSF Chimera 1.10.1. The different online drug assessment tools like Molinspiration (http://www.molinspiration.com/) and Molsoft (http://www.molsoft.com/) were employed to predict the drug-likeness and biological properties of these designed candidate molecules. The number of rotatable bonds, hydrogen bond acceptors (HBA) and hydrogen bond donors (HBD) were also confirmed by PubChem

(https://pubchem.ncbi.nlm.nih.gov/). Moreover, Lipinski's rule of five was analyzed using Molsoft and Molinspiraion tools.

2.6 Molecular docking of synthesized compounds using AutoDock

Molecular docking experiment study was done for all the synthesized ligands (6a-e) against urease using diverse AutoDock 4.2 tool according to the specified instructions[35]. In receptor (Carbonic anhydrase-II) the polar hydrogen atoms and Kollman charges were apportioned and for the ligand, Gasteiger partial charges were designated and non-polar hydrogen atoms were merged. All the torsion angles for all the synthesized ligands were set free to rotate through docking experiments. The docking experiments were performed by considering receptor as a rigid whereas ligands as flexible molecules. A grid map values were adjusted as of 80 Å x 80 Å x 80 Å on the targeted protein to generate the grid map (Figure S1). The number of docking runs for each docking experiment was set to 100 for the best conformational state. The Lamarckian genetic algorithm (LGA) and empirical free energy function were applied by taking docking parameters default. The docked complexes were further evaluated on lowest binding energy (Kcal/mol) values and hydrogen/hydrophobic bond analysis to choose the best docking pose using Discovery Studio (4.1) and UCSF Chimera 1.10.1.

3. Results and Discussion

3.1 Chemistry

The synthesis of amantadine drug derivatives has been outlined in scheme 1. Suitable substituted aromatic anilines were used precursors and the amine functionality of aniline was reduced by using method already reported in the literature. The diazonium salt formed after the reduction of

anilines was coupled with salicylaldehyde to construct azo linkage (4a-4e). The aldehyde functionality was utilized to obtain Schiff bases with amantadine as core nucleus **6a-6e**.

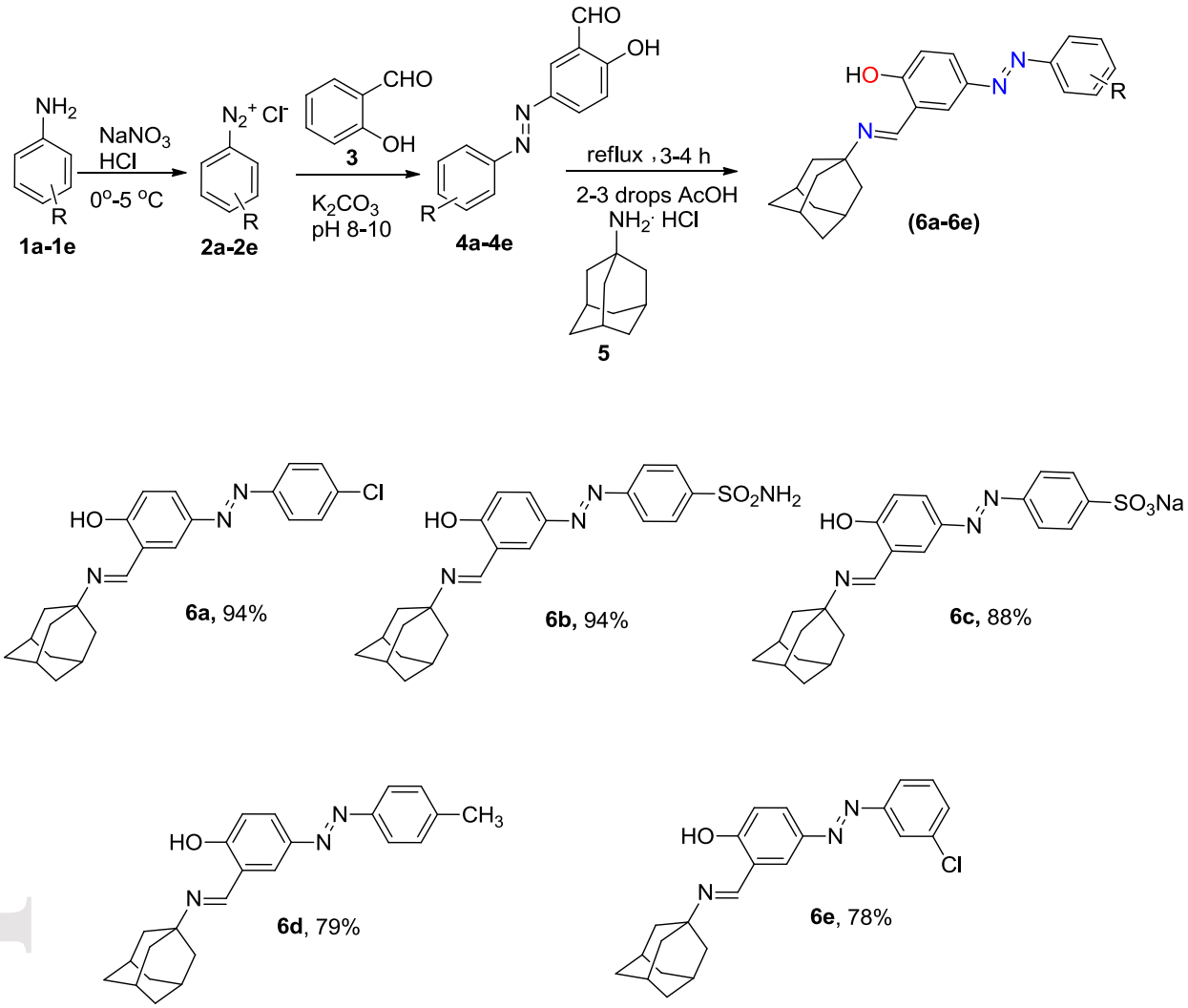

Scheme 1. Synthetic route towards salicylaldehyde based azo dyes and their condensation with adamantine **(6a-6e)**

The synthesized compounds were characterized through spectroscopic and elemental analysis. ^{1}H-NMR spectra revealed the formation of compounds and tentative signal assignments confirmed the newly constructed linkages. The characteristic imine proton appeared at around 8.5-9.5ppm value. The appearance of signals at 7-8 ppm value was attributed with the phenyl ring. The sp^3 carbons of amantadine show a slight variation in chemical environment and were observed at around 2-3 ppm value. ^{13}C-NMR spectra showed the presence of an isochronous carbons in compounds. The carbon of imine moiety appeared at around 165-170 ppm value. The appearance of signals at around 120-140 ppm were attributed to aryl ring and sp^3 carbons appeared at 18-28 ppm value (Figure S2 and S3).

3.2 Carbonic anhydrase II assay

The results of carbonic anhydrase enzyme inhibition activity are summarized in Table 1. All the synthesized derivatives **6a-6e** exhibited CA II inhibition in micromolar range and better than the standard used (Acetazolamide 0.9975±0.0489µM) except **6d**. Compound **6d** showed poor activity compared to other derivatives. **6d** contains a methyl group at the para position of the phenyl ring and methyl group exerts electron donating effect through hyperconjugation. The derivative **6b** and **6e** were found to be more potent compared to other derivatives in the series.

Table 1. Carbonic anhydrase activity (IC_{50} µM) of compounds (6a-6e)

6a	0.20 ± 0.01
6b	0.084 ± 0.002
6c	0.144 ± 0.006
6d	6.64 ± 0.33
6e	0.043 ± 0.002
Acetazolamide	0.99 ± 0.04

For calculation of $IC_{50,}$ six to eight concentrations were used. IC_{50} values were calculated by nonlinear regression using GraphPad Prism 5.0.

The higher potency of compound **6b** can be rationalized as depicted in Figure 3. The amino group of sulfonamide linked at the para position of phenyl ring forms the tetrahedral complex with the active site of carbonic anhydrase enzyme.

<<Insert Figure 3>>

Compound **6e** showed most significant carbonic anhydrase inhibition and it bears chlorine atom at meta position of phenyl ring which is involved in the charge separation through negative inductive effect. The aryl ring was tailored with a hydroxyl group which resulted in enhancement of inhibition by showing interactions with histidine residue of carbonic anhydrase enzyme (Figure 4).

<<Insert Figure 4>>

The overall carbonic anhydrase inhibition activity order was found to be in the following order

m-chloro> p-SO_2NH_2>SO_3Na>p-chloro>p-methyl

3.3 Chemo-informatics properties and Lipinski Rule (RO5) evaluation of ligands

The designed ligands were analyzed computationally to predict the best ligand on the basis of chemical and bio-molecular properties and RO5. The predicted chemo-informatics properties like Log*P*, HBD, HBA, molar volume, polar surface area (PSA) and drug-likeness values of ligand molecules are mentioned in Table 2. It has been confirmed from previous research data that the standard values for molecular weight (MW) and polar surface area (PSA) are (160 to 480 g/mol) and (<89 $Å^2$) respectively [22, 23]. The predicted results of compounds (6a-e) showed

good, MW and PSA values which are comparable with standard values. RO5 also confirmed the therapeutic potential of all the ligands. Hydrogen-bonding capacity has been identified as an important parameter for describing drug permeability. Research data revealed poor permeation is more likely to be observed when the HBA and HBD are exceeded than 10 and 5 respectively [24]. The chemo-informatics analysis justified that all the designed compounds possess <10 HBA and <5 HBD. Moreover, their log*P* values were also comparable with the standard value. However, there are plenty of examples available for RO5 violation amongst the existing drugs [25, 26]. The predicted chemo-informatics values of all the designed ligand are mentioned in Table 2.

Table 2. Chemo-informatics analysis of designed chemical compounds

Ligands	**Mol. Wt(g/mol)**	**No. HBA**	**No. HBD**	**Mol. Log*p*(mg/L)**	**PSA (A^2)**	**Mol.Vol (cm^3)**	**Drug Score**
6a	395.18	2	3	5.70	48.77	377.75	-0.02
6b	440.19	5	5	3.81	99.37	407.55	-0.34
6c	460.50	4	5	3.70	90.37	405.50	-0.32
6d	375.23	2	3	5.40	48.77	381.50	-0.58
6e	395.18	2	3	5.71	48.77	377.83	-0.20

Abbrevation: HBA= No of hydrogen bond acceptor, HBD= No of hydrogen bond donor, Log*P*= lippophilicity of partition coefficient, LogS= lippopilicity of water, PSA= polar surface area, MR=Molar refractivity, PZ=polarizability

3.4 Molecular docking and binding energy analysis

The docked complexes of all the compounds **6a-e** against carbonic anhydrase II were analyzed separately and evaluated on the basis of minimum energy values and ligand interactions pattern.

Results showed that all compounds **6a-e** showed good binding energy value -4.62, -5.04, -5.21, -4.65 and -5.44 kcal/mol, respectively and exhibited in the active region of the target protein (Table. 3). Prior research showed that the standard error for Autodock is testified as 2.5 kcal/mol. However, in all docking complexes, the predicted energy values difference was less than standard energy value. Although, the basic nucleus of all the synthesized compounds was similar, therefore most of the ligands possess good efficient energy values and have no big energy fluctuations difference. The comparative docking analysis and inhibition constant (IC_{50}) value justified that **6b** has good therapeutic potential as compared to all other compounds.

Table 3. Docking results of synthesized compounds using AutoDock

Ligands	**Binding energy (kcal/mol)**	**Ligand efficiency**	**Inhibition constant (uM)**	**Intermoleculr energy (kcal/mol)**	**Electrostatic energy (kcal/mol)**	**Torsional energy (kcal/mol)**
6a	-4.62	-0.13	270.21	-6.01	-0.16	2.39
6b	-5.04	-0.16	202.98	-7.13	0.02	2.09
6c	-5.21	-0.19	150.85	-6.70	0.10	1.49
6d	-4.65	-0.17	388.95	-6.14	0.01	1.49
6e	-5.44	-0.19	102.69	-6.93	-0.07	1.49

3.5 Binding analyses of synthesized compounds against carbonic anhydrase II

The ligands-protein binding analyses showed that **6b** confined in the active binding pocket of the target protein as mentioned in Figure 5. The CA II has an active site cleft (15 Å in diameter and 15 Å deep), and contains a $Zinc^{2+}$ ion that is coordinated in a tetrahedral geometry with three histidine residues (His94, His96 and His119) and a water molecule/hydroxide ion[27]. The **6b**-receptor docked complex reveals the best conformational state with hydrogen bond interactions within the receptor binding pocket. The docking result of **6b**-receptor docked complex showed

that two hydrogen bonds were observed at His93 and Ser1 residues respectively. The oxygen moiety of functional group in **6b** interacts with His93 with bond distance 3.51Å while OH group on benzene ring form another hydrogen bond against Ser1 with bond length 2.06Å respectively (Figure 5). No π-π stacking interactions were observed between ring structure of ligands and aromatic residues. The 2D conformations and binding pose and interactions with binding residues of all the candidate molecules are mentioned in (Figure. S4-S7)

<<Insert Figure 5>>

3. Conclusions

A large number of isoforms of carbonic anhydrase enzyme provide an incentive to design and develop safe and effective inhibitors. The use of hybrid pharmacophore approach is one of the key strategy in modern 4D (drug design discovery and development). In this account, we utilized hybrid pharmacophore approach by incorporating phenolic azo Schiff bases in amantadine drug. Azo and imine moieties were combined with amantadine drug. The synthesized derivatives 6a-6e were subjected to carbonic anhydrase and antioxidant activity. The derivative **6b** and **6e** were found to significant derivatives and showed better potential than the standard acetazolamide. The compound **6b** showed great therapeutic potential and exhibited good drug score -0.34. The docking result of **6b**-receptor docked complex showed that two hydrogen bonds were observed at His93 and Ser1 residues respectively. RO5 also confirmed the therapeutic potential of all the ligands. Hydrogen-bonding capacity has been identified as an important parameter for describing drug permeability. The results of carbonic anhydrase enzyme inhibition suggest that these synthesized derivatives can serve as structural templates in drug designing and discovery.

Conflict of Interest

Authors declare no any conflict of interest

List of figures legend, manuscript file

Figure 1. Mechanism of action of carbonic anhydrase

Figure 2. Some potent carbonic anhydrase inhibitors containing sulfonamides and sulfamates.

Figure 3. Amino group of **6b** interacts with zinc ions associated with histidine units

Figure 4. Hydroxyl group showing interactions with histidine residue

Figure 5. Docking interaction **6b** with the receptor molecule. **A**) The protein structure is represented in grey color while the interacted residues are justified in light maroon color. **B**) The closer view of binding interaction. The ligand molecule is depicted in purple color while their functional groups such as oxygen, nitrogen and sulfur are shown in red, blue and yellow colors respectively. Amino acids are highlighted in maroon color and purple dotted lines justify the hydrogen binding with distance mentioned in angstrom (Å). Two hydrogen bonds were observed at His93 and Ser1 position in the target protein. Zinc metal is represented in the grey circle.

List of figure legends of supplementary information file

Figure.S1 A) Crystal structure of bovine anhydrase II. **B)** Ramachandran graph accessed from PDB.

Figure S2 ^{13}C-NMR spectrum of 6b

Figure S3 ^{1}H-NMR spectrum of 6b

Figure S4. Docking 6a against target protein

Figure S5. Docking 6c against target protein

Figure S6. Docking 6d against target protein

Figure S7. Docking 6e against target protein

References

[1]. Supuran, C.T., 2008. Carbonic anhydrases: novel therapeutic applications for inhibitors and activators. *Nat. Rev Drug Disc*, **2008**, 7, 181.

[2]. Hu, J., Fu, R., Cross, T.A., *Biophys J*. **2007**, 93, 283.

[3]. Cady, S.D., Schmidt-Rohr, K., Wang, J., Soto, C.S., DeGrado, W.F., Hong, M. *Nature*, **2010**, 463, 692.

[4]. Rogoz, Z., Skuza, G., Daniel, W.A., Wójcikowski, J., Dudek, D., Wróbel, A., *Pharmacol Rep*, **2007**, 59, 778.

[5]. Camps, P., Duque, M.D., Vázquez, S., Naesens, L., De Clercq, E., Sureda, F.X., López-Querol, M., Camins, A., Pallàs, M., Prathalingam, S.R., Kelly, J.M., *Bioorg. Med. Chem*. **2008**, 16, 9936.

[6]. Garaj, V., Puccetti, L., Fasolis, G., Winum, J.Y., Montero, J.L., Scozzafava, A., Vullo, D., Innocenti, A. and Supuran, C.T., *Bioorg. Med Chem. Lett*. **2004**, 14, 5433.

[7]. Esirden, İ., Tanç, M., Supuran, C.T., Kaya, M., *Bioorg. Med. Chem. Lett*, **2017**, 27, 89.

[8]. Smirnovienė, J., Smirnovas, V., Matulis, D., *Anal. Biochem*, 522 (2017) 61-72.

[9]. Gündüzalp, A.B., Parlakgümüş, G., Uzun, D., Özmen, Ü.Ö., Özbek, N., Sarı, M., Tunç, T., *J. Mol. Struct*. **2016**, 1105, 340.

[10]. Imran, S., Taha, M., Ismail, N.H., Fayyaz, S., Khan, K.M., Choudhary, M.I., *Bioorg. Chem*, **2016**, 68, 104.

[11]. Altıntop, M.D., Sever, B., Özdemir, A., Kucukoglu, K., Onem, H., Nadaroglu, H., Kaplancıklı, Z.A., *Bioorg. Med. Chem*. **2017**, 25, 3554.

[12]. Eldehna, W.M., Al-Ansary, G.H., Bua, S., Nocentini, A., Gratteri, P., Altoukhy, A., Ghabbour, H., Ahmed, H.Y., Supuran, C.T., *Eur. J. Med. Chem*. **2017**, 127, 530.

[13]. Sethi, K.K., Vullo, D., Verma, S.M., Tanç, M., Carta, F., Supuran, C.T., *Bioorg. Med. Chem*. **2013**, 21, 5982.

[14]. Fattah, T.A., Saeed, A., Channar, P.A., Larik, F.A., Hassan, M., Raza, H., Abbas, Q. Seo, S.Y., 2018. *Drug Res*. **2018**, DOI https://doi.org/10.1055/s-0043-123998

[15]. Vicini, P., Geronikaki, A., Incerti, M., Busonera, B., Poni, G., Cabras, C.A., La Colla, P., *Bioorg. Med. Chem*, **2003**, 11, 4789.

[16]. Desai, S.B., Desai, P.B., Desai, K.R., *Heterocyclic Commun*, **2001** 7, 90.

[17]. Bharti, S.K., Nath, G., Tilak, R. Singh, S.K., *Eur. J. Med. Chem*, **2010** 45, 660.

[18]. Qin, W., Long, S., Panunzio, M., Biondi, S., *Molecules*, **2013**, 18, 12289.

[19]. Jarrahpour, A.A., Motamedifar, M., Pakshir, K., Hadi, N., Zarei, M., *Molecules*, **2004** 9, 824.

[20]. Przybylski, P., Huczynski, A., Pyta, K., Brzezinski, B., Bartl, F., Curr. *Org. Chem*. **2009**, 13, 148.

[21]. Ispir, E., Dyes. *Pigm*. **2009**, 82, 19.

[22]. Kadam, R.U, Roy N, *Indian. J. Pharma Sci*. **2007** 69, 615.

[23]. Ghose AK, Herbertz T, Hudkins RL, Dorsey BD and Mallamo JP. *ACS Chem. Neurosci*. **2012**, 3, 68.

[24]. Bakht, M.A, Yar, M.S, Abdel-Hamid S.G, Al-Qasoumi S.I, Samad A., *Eur. J. Med. Chem,* **2010** 45, 5869.

[25]. Tian S, Wang J, Li Y, Li D, Xu L, Hou T. *Adv. Drug. Deliv. Rev*, **2015**, 86, 2–10.

[26]. Prerana B. Jadhav, Akshay R.Yadav and Megha G. Gore. *Int. J. Pharm. Bio. Sci,* **2015**, 6, 154.

[27]. C.T. Supuran, *Nat. Rev. Drug Discov*, 2008 7, 181.

[28]. al-Rashida, M., Ashraf, M., Hussain, B., Nagra, S.A., Abbas, G., *Bioorg. Med. Chem*, **2011**, 19, 3371.

[29]. a) Larik, F.A., Saeed, A., Channar, P.A., Muqadar, U., Abbas, Q., Hassan, M., Seo, S.Y. Bolte, M., *Eur. J. Med. Chem*, **2017**, 141, 281. b) Larik, F.A., Saeed, A., Channar, P.A., Ismail, H., Dilshad, E. Mirza, B., *Bangladesh. J. Pharmacol*. **2016**, 11, 902.

[30]. Pettersen, E.F, Goddard, T.D, Huang C.C, Couch G.S, Greenblatt D.M, Meng E.C, Ferrin T.E. *J. Comput. Chem*. **2006**, 25, 1612.

[31]. Lovell SC, Davis IW, Arendall WB 3rd, de Bakker PI, Word JM, Prisant MG, Richardson JS, Richardson DC. *Proteins*. **2002** 50, 450.

[32]. Chen VB, Arendall WB 3rd, Headd JJ, Keedy DA, Immormino RM, Kapral GJ, Murray LW, Richardson JS, Richardson DC. *Acta Crystallogr D Biol Crystallogr*. **2016** 66, 21.

[33]. Studio, Discovery. "Version 2.1." *Accelrys: San Diego, CA* **2008**.

[34]. Willard L, Ranjan A, Zhang H, Monzavi H, Boyko RF, Sykes BD, Wishart DS. *Nucleic. Acids. Res*. **2003**, 31, 3319.

[35]. Morris G.M, Huey R, Lindstrom W, Sanner MF, Belew R.K, Goodsell D.S, Olson A.J. *J. Comput. Chem.* **2009**, 30, 2791.